Cane et al., http://www.jcb.org/cgi/content/full/jcb.201211119/DC1

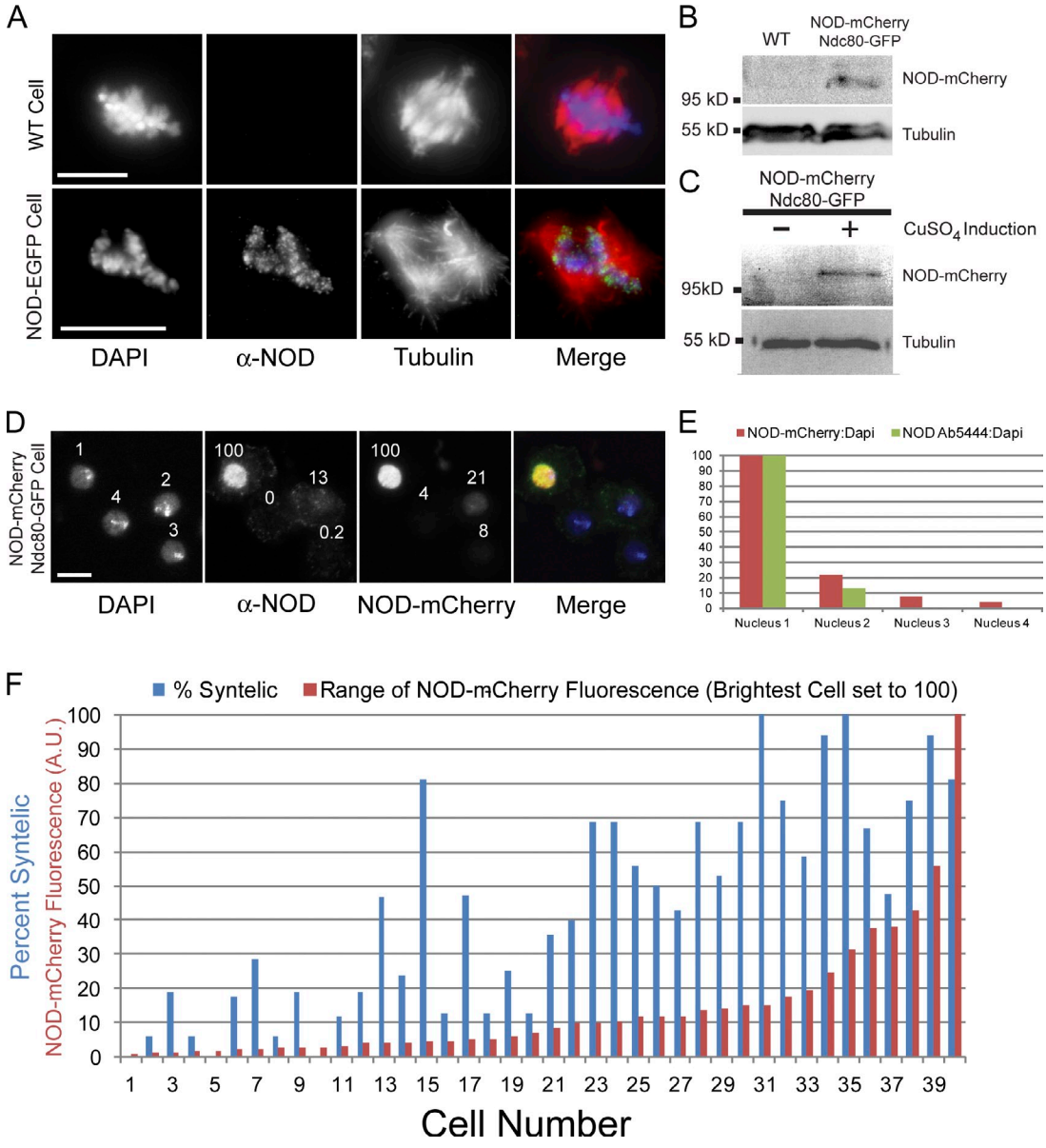

Figure S1. **Characterization of a polyclonal NOD antibody and examination of NOD-mCherry expression levels.** (A) IF with polyclonal NOD antibody 5444 of wild-type and NOD-EGFP–expressing cells. Exogenous NOD-EGFP but not endogenous NOD is detectable by IF with the NOD antibody. In the merged images DNA is blue, anti-NOD staining is green, and tubulin is red. (B and C) NOD antibody 5444 specifically recognizes a 105-kD band by Western blot analysis of S2 cell extracts from induced NOD-mCherry–expressing cells. (D) NOD antibody 5444 recognizes NOD-mCherry in high-expressing cells. The number above each nucleus is the fluorescence intensity relative to the brightest cell in the field, which was set to 100. In the merged image DNA is blue, anti-NOD staining is green, and NOD-mCherry signal is red. Because the cells are in interphase, there is no centromere/kinetochore localized Ndc80-GFP. (E) Quantification of NOD-mCherry and NOD IF signal from the four nuclei shown in D. mCherry signal detection is more sensitive than detection of NOD-mCherry by IF. The antibody cannot detect NOD-mCherry levels that are below 10% of the highest NOD-mCherry–expressing cell in the field. (F) Plot of percentage of syntelic and NOD-mCherry fluorescence for 40 different cells. Stable syntelic attachments, which are extremely rare in S2 cells (~0.2–0.5% of all attachments), are observed even in cells expressing the lowest detectable levels of NOD-mCherry (~1% of the maximum NOD-mCherry–expressing cell in the data set). Bars, 10 µm.

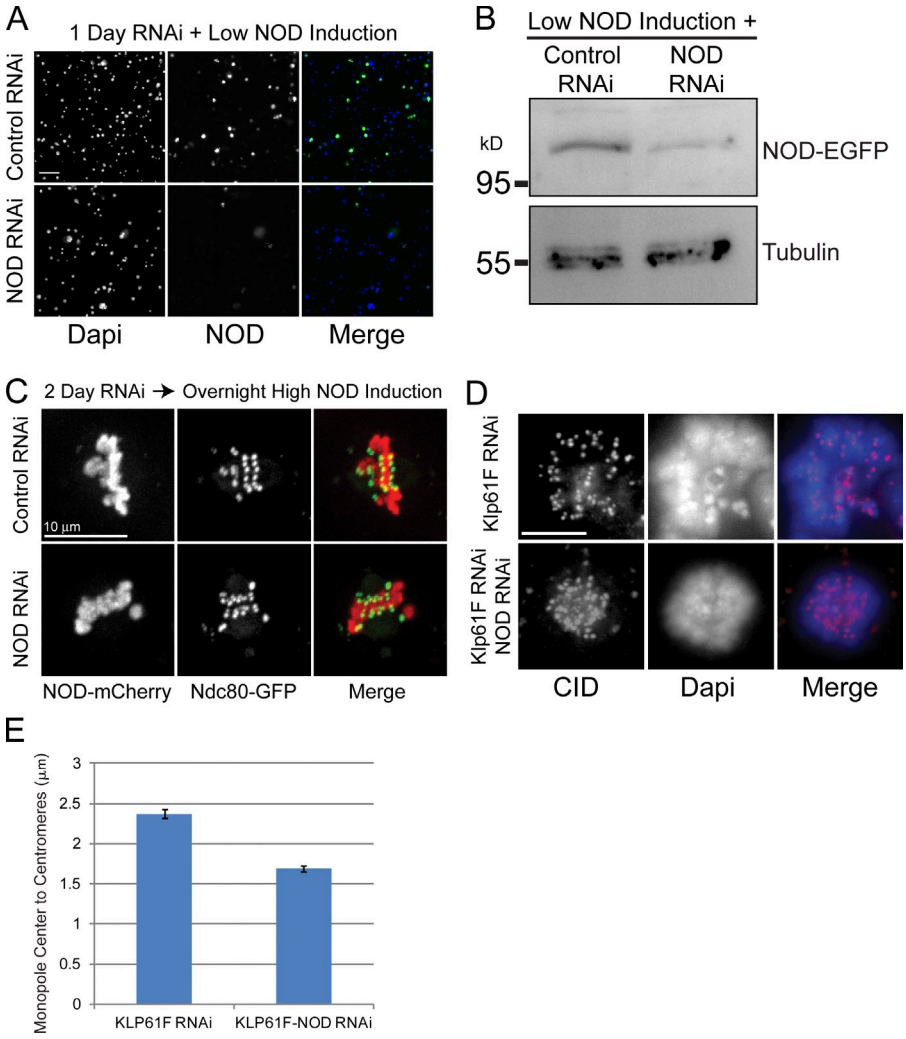

Figure S2. **NOD generates an away-from-the-pole force in S2 cells and the NOD overexpression phenotype is not caused by a dominant-negative effect.** (A) Treatment with NOD dsRNA for 1 d significantly reduces low induction of NOD-EGFP (25 µM $CuSO_4$). (B) Western blot of cell extracts prepared from the cells shown in A blotted with anti-GFP serum (top) and anti-tubulin antibody (bottom) as a loading control. (C) Stable syntelic attachments are observed after overnight high NOD-mCherry induction (500 µM $CuSO_4$) in cells treated with dsRNA targeting endogenous NOD for 2 d. (D) Centromeres (CID) move closer to the center of monopolar spindles assembled in the absence of Klp61F (kinesin-5) when NOD is depleted by RNAi. (E) Quantification of the distance between the monopole center and CID-stained centromeres. The distance between CID-stained centromeres and monopole centers decreased by 30% in the absence of NOD (n = 468 centromeres for control RNAi and 491 centromeres for NOD RNAi). Bars: (A) 50 µm; (C) 10 µm; (D) 5 µm. Error bars represent the SEM.

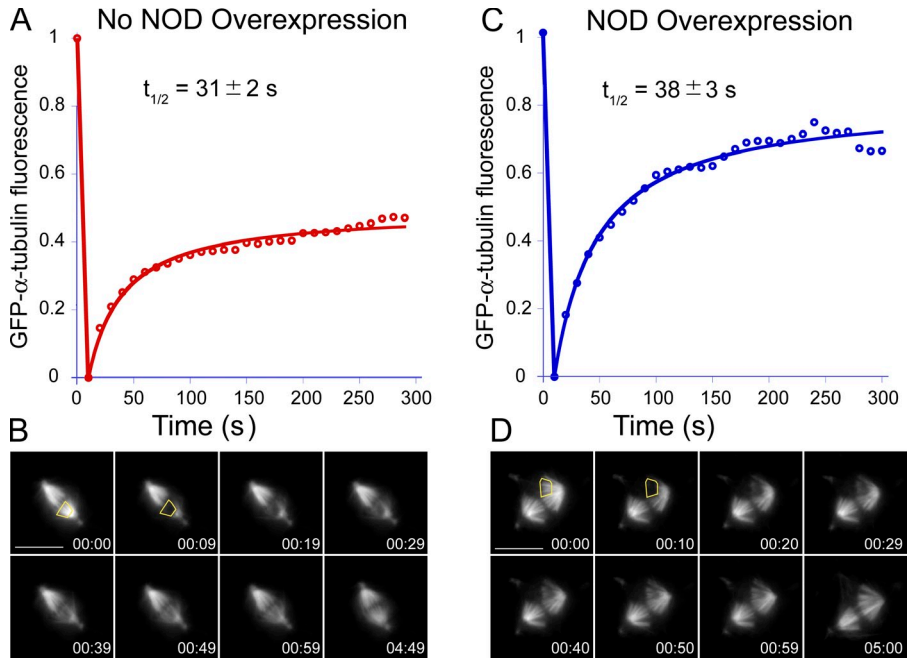

Figure S3. **FRAP measurements of GFP–α-tubulin turnover in control and high NOD-expressing cells.** Regions near the spindle equator (yellow outline in B and D) of control cells (*n* = 8 cells; A) or NOD-mCherry expressing cells (*n* = 8 cells; C) were bleached and the cells were imaged every ~10 s for ~5 min. The fluorescence intensity in the bleached regions was quantified over time and the recovery data were plotted and fit with a hyperbolic function—y = (x*m2)/(m1 + x)—to define a $t_{1/2}$. The $t_{1/2}$ values were measured to be 31 ± 2 s for control cells and 38 ± 3 s for NOD-mCherry–expressing cells. These values reflect the rapid turnover of nonkinetochore microtubules in the spindle. The difference in percent recovery between control and NOD-mCherry–expressing cells is a result of excessive bleaching of the soluble pool of tubulin in control cells, which was approximately two times higher than in NOD-mCherry–expressing cells. The R value for both curve fits is 0.99.

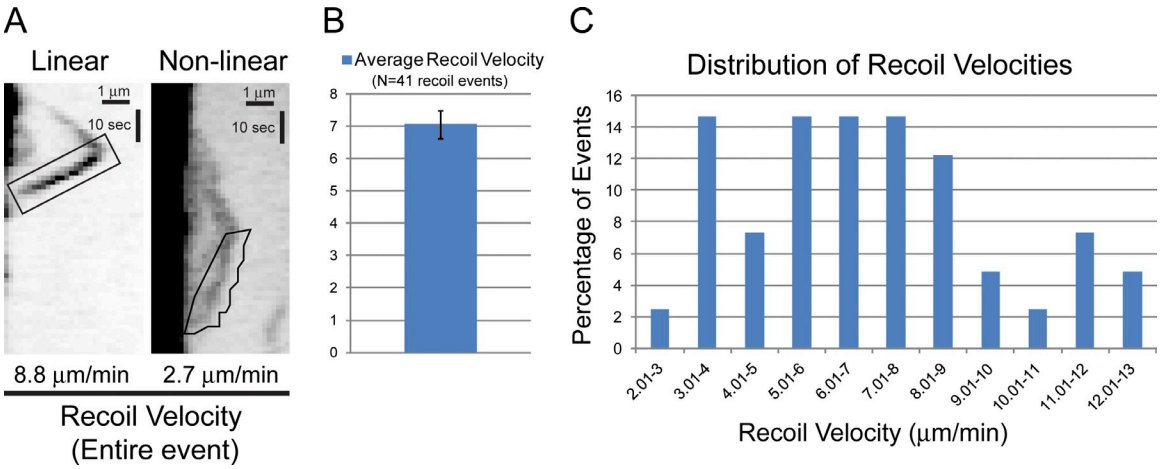

Figure S4. **Chromatin recoil velocities are variable.** (A) Kymographs of stretch events with the recoil phase outlined. Some recoil events are linear with a constant velocity, whereas others are nonlinear with a nonuniform velocity. Velocities shown are for the entire recoil event. (B) The mean recoil velocity was measured at 7.1 µm/min (*n* = 41 events). (C) A broad range of recoil velocities between ~2 and ~12 µm/min were observed. Error bars represent the SEM. Bars, 1 µm (horizontal) and 10 s (vertical).

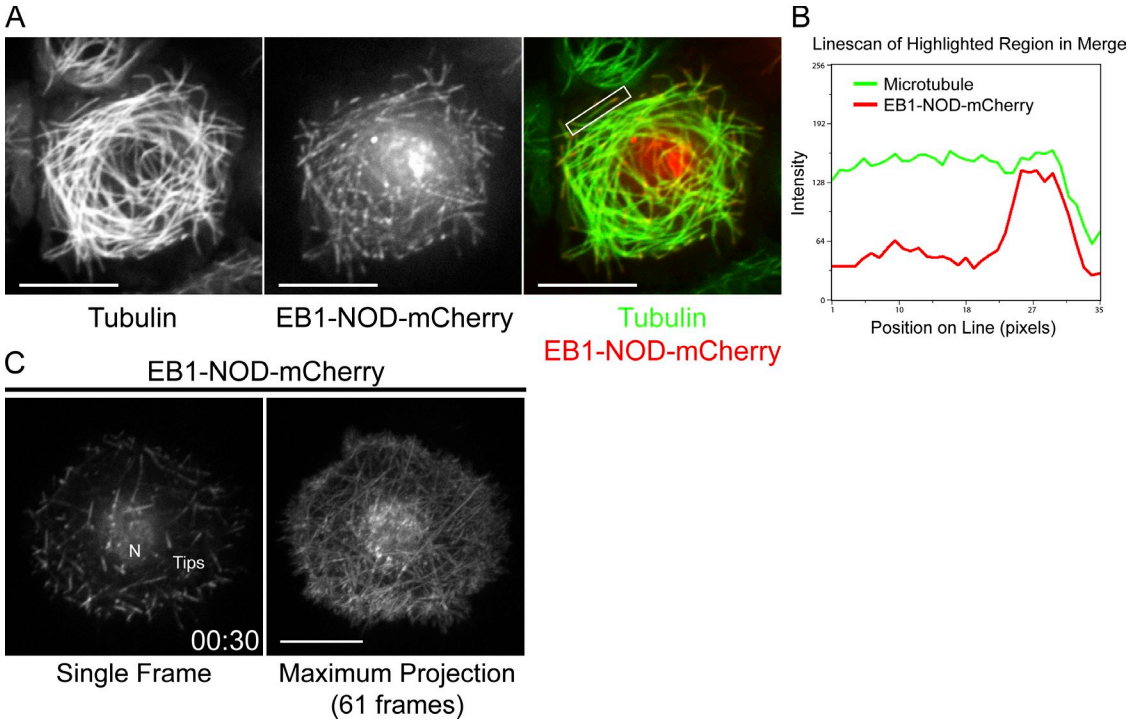

Figure S5. **EB1-NOD-mCherry tip tracks along polymerizing microtubules in interphase cells.** (A) Selected frame from a confocal time lapse of a GFP–α-tubulin (green)– and EB1-NOD-mCherry (red)–expressing S2 cell in interphase. (B) Line scan of the microtubule highlighted (box) in the merged image in A shows the enrichment of EB1-NOD-mCherry (red line) at the plus end of the microtubule (green line). (C) EB1-NOD-mCherry localizes to both the nucleus (N) and the cytoplasm. The cytoplasmic pool of EB1-NOD-mCherry localizes to the ends of growing microtubules (Tips). The trajectories of polymerizing microtubules are evident in the maximum intensity projection of EB1-NOD-mCherry from a confocal time lapse. Bars, 10 µm.

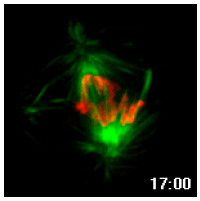

Video 1. **S2 cell expressing GFP–α-tubulin and NOD-mCherry.** Frames were acquired at 1-min intervals on a TE300 inverted microscope with a CSU10 spinning disk confocal head and an Orca ER camera. The cell advances from metaphase to anaphase despite the presence of a misaligned chromosome in which both sister chromatids are attached to the same pole. During anaphase both sisters move toward the same pole resulting in two aneuploid daughter cells. Elapsed time is minutes:seconds. Bar, 10 µm.

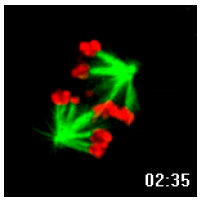

Video 2. **S2 cell expressing GFP–α-tubulin and NOD-mCherry.** Frames were acquired at 5-s intervals on a TE300 inverted microscope with a CSU10 spinning disk confocal head and an Orca ER camera. This high NOD-mCherry–expressing cell has numerous misaligned chromosomes in which the sister chromatids are stably attached to the same pole. Elapsed time is minutes:seconds. Bar, 10 µm.

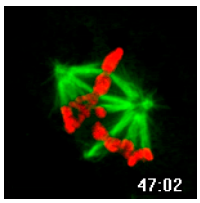

Video 3. **S2 cell expressing GFP–α-tubulin and NOD-mCherry.** Frames were acquired at 1-min intervals on a TE300 inverted microscope with a CSU10 spinning disk confocal head and an Orca ER camera. The cell establishes a mixture of incorrect kt-MT attachments within 5–10 min of nuclear envelope breakdown and the aberrant attachments persist for the duration of mitosis, with the exception of a monooriented chromosome that initiates polymerization of a k-fiber (beginning at 09:00) that forms a third spindle pole. Despite the presence of numerous incorrectly attached chromosomes, the cell enters anaphase 90 min after nuclear envelope breakdown. Elapsed time is minutes:seconds. Bar, 10 µm.

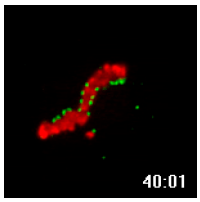

Video 4. **S2 cell expressing Ndc80-GFP and NOD-mCherry.** Frames were acquired at 1-min intervals on a TE300 inverted microscope with a CSU10 spinning disk confocal head and an Orca ER camera. Bioriented and syntelic attachments are apparent in the center and periphery of the chromosome mass, respectively. Juxtaposed sister kinetochores (Ndc80-GFP) facing the same pole is the hallmark of syntelic attachments. With the exception of a clear instance of a bioriented chromosome transitioning to a syntelic attachment (between 20 and 22 min) the attachment states persist for the duration of the time lapse (76 min). Elapsed time is minutes:seconds. Bar, 10 µm.

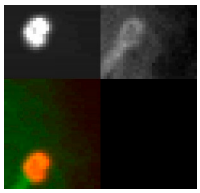

Video 5. **S2 cell expressing Ndc80-GFP and NOD-mCherry.** Frames were acquired at 5-s intervals on a TE300 inverted microscope with a CSU10 spinning disk confocal head and an Orca ER camera. The chromosome seen in this video is attached to the spindle pole through k-fibers (bottom left) and undergoes three chromatin stretching events. The first stretch event (between 00:05 and 00:30) is rapid and is associated with a microtubule that polymerizes past the chromatin and then stalls and buckles as the chromatin recoils. The separation between the plus end of the microtubule (open arrowhead) and the stretched chromatin (closed arrowhead) at t = 15 s is a consequence of sequential imaging. A persistent stretch event occurs between 01:15 and 01:50 of the time lapse. The microtubule, which initially extends past the chromosome, makes a glancing interaction with the chromosome. Upon contact, the chromatin stretches (closed arrowhead) toward the dynamic plus end (open arrowhead) and persists until it retracts coincident with the shrinking microtubule. Another rapid stretch event takes place between 02:20 and 02:30. Elapsed time is minutes:seconds. Bar, 1 µm.

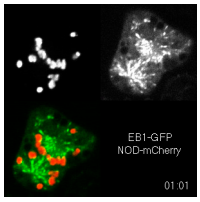

Video 6. **S2 cell expressing EB1-GFP and NOD-mCherry.** Frames were acquired at 2-s intervals on a TiE inverted microscope with a CSU-X1 spinning disk confocal head and an iXON EMCCD camera. Elapsed time is minutes:seconds. Bar, 10 µm.

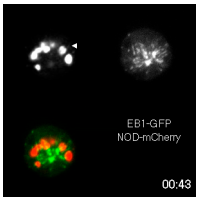

Video 7. **S2 cell expressing EB1-GFP and NOD-mCherry.** Frames were acquired at 2-s intervals on a TiE inverted microscope with a CSU-X1 spinning disk confocal head and an iXON EMCCD camera. The arrowhead between 0:38 and 0:49 (top left) highlights the rapid stretch event that is shown in the kymograph in Fig. 7 C. Elapsed time is minutes:seconds. Bar, 10 µm.

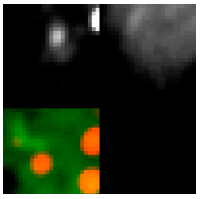

Video 8. **S2 cell expressing EB1-GFP and NOD-mCherry.** Frames were acquired at 2-s intervals on a TiE inverted microscope with a CSU-X1 spinning disk confocal head and an iXON EMCCD camera. The arrowhead (top left) highlights a NOD-mCherry fragment that is propelled through the cytoplasm and colocalizes with an EB1-GFP comet (top right). NOD-mCherry is in red and EB1-GFP is in green in the merged time lapse (bottom left). This event is represented in the kymograph shown in Fig. 7 D. Elapsed time is minutes:seconds. Bar, 1 µm.

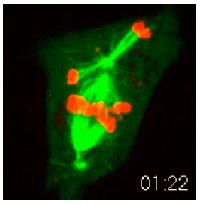

Video 9. **S2 cell expressing GFP–α-tubulin and NOD-mCherry.** Frames were acquired at 2-s intervals on a TiE inverted microscope with a CSU-X1 spinning disk confocal head and an iXON EMCCD camera. The arrowhead between 1:28 and 3:01 highlights the end-tracking event that is shown in the kymograph in Fig. 7 G. The right panel shows an 8× zoom of the region where the end-tracking event occurred. Elapsed time is minutes:seconds. Bars: (left) 10 µm; (right) 1 µm.

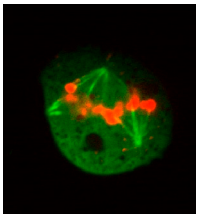

Video 10. **S2 cell expressing GFP–α-tubulin and kinesin-1-NOD-mCherry.** Frames were acquired at 5-s intervals on a TiE inverted microscope with a CSU-X1 spinning disk confocal head and an iXON EMCCD camera. Note the extensive stretching of the chromatin in the kinesin-1-NOD-mCherry channel (right).